Fuel 236 (2019) 589–597

Contents lists available at ScienceDirect

Fuel

journal homepage: www.elsevier.com/locate/fuel

Full Length Article

Novel route of synthesis of ultra-small Au nanoparticles on SiO_2 supports

Y. Kotolevich[a,*], O. Martynyuk[a], S. Martínez-González[b], H. Tiznado[a], A. Pestryakov[c], M. Avalos Borja[d], V. Cortés Corberán[b], N. Bogdanchikova[a]

[a] Centro de Nanociencias y Nanotecnología, Universidad Nacional Autónoma de México, Km. 107 Carretera Tijuana-Ensenada, 22860 Ensenada, Mexico
[b] Institute of Catalysis and Petroleumchemistry (ICP), CSIC, Marie Curie 2, 28049 Madrid, Spain
[c] Tomsk Polytechnic University, Lenin Avenue 30, Tomsk 634050, Russia
[d] Instituto Potosino de Investigación Científica y Tecnológica, División de Materiales Avanzados, 78216 San Luis Potosí, S.L.P., Mexico

ARTICLE INFO

Keywords:
1 nm gold nanoparticles
Metal nanoparticles synthesis
Ultra-small silica
1-Octanol oxidation
Gold electronic states

ABSTRACT

A novel route to prepare monodispersed 1–2 nm gold nanoparticles (NPs), based on the use of extremely small SiO_2 NPs (2–4 nm) as a support and increasing their metal-support interaction with surface modifier oxides is presented. The influence of modifier (La, Ce and Fe oxides) and modification method (impregnation (*i*) or direct synthesis (*s*)) on the formation of ultra-small Au NPs and their structural and electronic properties was studied. The samples were characterized by N_2 adsorption (BET), FTIR of adsorbed CO, XRD and HR-TEM methods, and tested for the catalytic selective oxidation of 1-octanol. Preparation of monodispersed Au NPs with 1 nm diameter was successfully achieved for all the modified samples studied, with exception of Au/Ce/SiO_2-*i*, where CeO_2 was not homogeneously distributed. The Au NPs have high degree of monodispersity and are stable when treated in H_2 up to 300 °C. Formation of these Au NPs depended on the strong interactions between the cationic gold complex precursor and the surface of modified SiO_2 NPs. Modifiers changed electronic properties of supported gold; favoring the formation and stabilization of $Au^{\delta+}$ states, which are probable gold active sites of selective liquid-phase oxidation of alcohols in redox catalytic processes. 1-octanol oxidation was used as a model reaction for oxidation of fatty alcohols obtained during biomass transformation. The best performance for 1-octanol oxidation was found for gold nanoparticles supported on the ultra-small SiO_2 modified cerium oxide by impregnation method. The relative order of activity was: AuCeSiO_2-*i* > AuFeSiO_2-*i* ≫ AuLaSiO_2-*i* ≈ AuLaSiO_2-*s* > AuSiO_2 > AuFeSiO_2-*s* ≫ AuCeSiO_2-*s*. The obtained results open the possibility of further development of high-performance catalysts for conversion of secondary products of biomass processing into valuable chemicals.

1. Introduction

Small gold nanoparticles (Au NPs) are widely used in catalysis [1–3], medicine [4–6], sensors [7–10], optoelectronic devices [11] and others [12]. Much effort has been made to elucidate the correlation between Au NPs size and their catalytic properties [2,3,8]. Thus, obtaining monodisperse gold nanopowders and supported Au NPs is an important practical task, which is the subject of numerous recent scientific researches.

Gold nanoparticles attract great interest due to their high catalytic activity at room temperature [13–25]. For example, high monodispersity of Au NPs with size < 2 nm is one of the main factors of activity of gold catalysts in the processes of conversion of fatty and polyatomic alcohols, by-products of biomass transformation to biodiesel [26–33]. In the synthesis of supported Au NPs the nature of support is an important factor for their functionality. Synthesis of small monodispersed Au NPs on inert supports such as SiO_2, Al_2O_3, etc. is very complicated due to the weak metal-support interaction and the consequent ease of sintering of the gold particles. The application of inert supports is extremely important for studying the mechanisms of catalytic reactions [34–38], since the use of active supports does not allow separating activity of different Au states from active support influence.

Literature search of synthesis of monodisperse Au NPs with diameter 1–2 nm on inert supports showed that the term «monodispersity» is frequently used even when the size corresponding to the maximum in the distribution histogram correspond to less than 50% of the total particle number [39–42]. To our opinion, the particles can be considered as monodispersed when the size of the particles varies not more than ± 10%.

One way to obtain monodisperse distribution of Au NPs with 1 nm size on SiO_2 was described in literature using the coating the surface of

* Corresponding author.
E-mail address: nina@cnyn.unam.mx (Y. Kotolevich).

https://doi.org/10.1016/j.fuel.2018.09.050
Received 15 March 2018; Received in revised form 29 August 2018; Accepted 7 September 2018

inert support with a layer of carbon with better metal-support interaction [43,44]. However, this method diverts us from obtaining gold nanoparticles on the surface of SiO_2. Au NPs with a size of 1 nm were synthesized by stabilizing them in a polymer capsule and then supporting them on SiO_2 [45]. Strictly speaking, the study of Au NPs properties in this system is impossible, because a stabilizing polymer can block Au nanoparticle surface. Modification of the support surface with different compounds, e.g., transition metal oxides, is one of the most effective methods to vary the structural and electronic properties of supported metals. Changes in electronic state (effective charge) of supported gold systems as a result of metal-support interaction are the main reason to use specifically supported Au NPs rather than free ones. According to our previous results, supported gold ions Au^+ and charged clusters $Au_n^{\delta+}$ are active sites of gold catalysts in oxidation processes [30–33,46,47]. So, synthesis of small supported Au NPs (1–2 nm) with high degree of the metal monodispersity is one of key factors to obtain highly effective catalysts for oxidation processes, including conversion of by-products of biomass.

Besides its potential for renewable energy, biomass accounts for huge amounts of new raw materials for chemicals production, including a vast source of alcohols due to fermentation, among others processes. In this regard, selective oxidation of fatty alcohols to the corresponding aldehydes, acids and esters, holds potential to open new paths for the synthesis of products with high added value for fine chemicals, though this type of alcohols are the most difficult to oxidize. Recent investigations conducted by our group have shown that catalytic oxidation of 1-octanol under demanding mild conditions, i.e. base-free, at low temperature and under atmospheric pressure, is very sensible to the nature and electronic state of supported Au NPs catalysts [30–33].

In the present paper we propose a new approach of synthesis of monodispersed small Au NPs (1–2 nm) on SiO_2 based on the application of ultra-small silica particles (d ~ 2 nm), described in our previous work [50]. Such particles have high surface energy and interact strongly with supported metal NPs. We investigated the regulation of properties of the supported Au NPs by addition of Fe, Ce and La oxides, which showed high efficiency in our previous studies [30–32]. The effects of modification of the synthesized samples on their structural, electronic and catalytic properties for selective oxidation of 1-octanol were studied.

2. Experimental

2.1. Supports preparation

Mesoporous silica was synthesized by a neutral S^0I^0 templating route (S^0: neutral primary amine surfactant; I^0: neutral inorganic precursor) as reported elsewhere [49,50]. Dodecylamine was employed as surfactant and mesitylene as swelling organic agent [51]. The reaction products were filtered, washed with distilled water, and dried at room temperature for 24 h and at 100 °C for 2 h. The template was then removed by calcination, increasing the temperature at a rate of 2.5 °C min^{-1} and maintaining it at 550 °C for 3.5 h in air.

Incorporation of the metal oxides (M) was carried out by two methods. In the first one, direct synthesis (denoted as *s*), the modifier metal oxide is incorporated in the synthesis of silica using cerium (III) nitrate hexahydrate, iron (III) nitrate nonahydrate or lanthanum (III) nitrate hexahydrate as precursors, with an atomic ratio Si/M = 40 (M = Fe, Ce, La). The reaction products were filtered, washed with distilled water, and dried at room temperature for 48 h, followed by drying at 110 °C for 4 h, and then the samples were calcined at 550 °C for 4 h in static air. In the second one, impregnation (denoted as *i*), the incorporation was done by incipient impregnation of the pure silica support using 1.5 cm^3/g of aqueous solution of the same M precursors used in the other method *(s)*, with the concentration needed to obtain a final molar ratio Si/M = 40. These impregnated samples were dried and calcined under the same conditions previously described for the direct synthesis method. Catalysts will be denoted hereinafter as Au/(M)/SiO_2-*x*, where M is the metal of the modifier oxide and ***x*** indicates the synthesis method (*s*: direct synthesis; *i*: impregnation).

2.2. Catalysts preparation

Commercial $HAuCl_4{\cdot}3H_2O$ (Aldrich, Saint Louis, MO, USA) was used as gold precursor. Gold complex $Au(en)_2Cl_3$ was synthesized as described elsewhere [33,52,53]. Briefly, ethylenediamine (en, 0.45 mL) was slowly added to $HAuCl_4{\cdot}3H_2O$ solution in deionized water (1.0 g of Au precursor in 10 mL) and washed with ethanol (70 mL). The precipitate produced was filtered and dried at 40 °C under vacuum overnight.

To prepare Au NPs on silica supports, $Au(en)_2Cl_3$ (0.5 g) was dissolved in water (50 mL) adjusting the pH to 10.0 by the addition of the aqueous solution of NaOH (5.0 wt%). Silica support (modified or unmodified) (1.0 g) was added and stirred at 60–70 °C for 2 h. The reaction products were filtered, washed with distilled water and dried in vacuum at 70 °C for 5 h. Finally, the materials were thermally treated at 300 °C in H_2 for 1.5 h to ensure a complete removal of the organic template.

2.3. Catalysts and supports characterization

Before characterization tests all bare supports and gold-containing samples were reduced in hydrogen flow, at 300 °C for 1 h. The textural properties were determined from nitrogen adsorption-desorption isotherms (−196 °C) recorded with a Micromeritics TriStar 3000 apparatus. Prior to experiments, samples were degassed at 300 °C in vacuum for 5 h. The volume of the adsorbed N_2 was normalized to a standard temperature and pressure. The specific areas (S_{BET}) of the samples were calculated by applying the BET method to the nitrogen adsorption data within the P/P_0 range 0.005–0.250.

Supports and gold-containing samples were characterized by powder X-ray diffraction (XRD) according to the step-scanning procedure (step size 0.02°; 0.5 s) with a Philips XPert PRO diffractometer, using Ni-filtered CuKα (λ = 0.15406 nm) radiation. Assignment of crystalline phases was based on the ICDD- 2013 powder diffraction database. Crystallite size and phase quantification was done by Rietveld refining, by using the X'Pert HighScore Plus software package from Malvern Panalytical. Crystalline size was a result of the refining using Debye-Scherrer formula.

High-resolution transmission electronic microscopy (HRTEM) studies were carried out using a JEM 2100F system operating with a 200 kV accelerating voltage. Gold and modifier contents were measured in the same system, equipped with a TermoNoran Super Dry, by energy dispersive spectroscopy (EDS).

Fourier transformed infrared spectra (FTIR) of CO adsorbed on the gold-containing samples surface were recorded in a Tensor 27 FTIR spectrometer (Bruker, Germany) in transmittance mode with a resolution of 4 cm^{-1}. *In situ* experiments were carried out in a quartz cell with NaCl windows capable of working at temperatures from −100 to 500 °C and pressures from 10^{-2} to 760 Torr. The sample powder was pressed into disks of 13 mm diameter and ca. 20 mg. The sample was pretreated in H_2 or O_2 (100 Torr) at 300 °C for 1 h and then cooled down to room temperature. It was chosen 300 °C to match the catalytic activity measurement temperature. Pretreatment in O_2 was used to model the influence of an oxidative atmosphere during the catalytic reaction. After that, H_2 or O_2 was evacuated and CO adsorption (Research grade, P^0 = 30 Torr, Matheson USA) was carried out. Spectra are presented after subtracting the CO gas phase background, previously recorded without sample, also at 30 Torr (blank).

For testing the catalytic properties, catalyst was added (in a substrate/metal ratio R = 100 mol/mol) to 20 mL of 1-octanol solution (0.1 M) in n-heptane, in a four-necked round bottom flask equipped with reflux condenser, oxygen feed, thermometer and a septum cap.

Table 1
Textural properties of sample and analytical composition of after H_2 treatment at 300 °C for 1 h.

Sample	Analytical Si/M atomic ratio	Analytical M content (wt%)	Analytical Au content (wt%)	S_{BET} (m^2/g)	
				Support	Catalysts
Au/SiO_2	–	–	2.51	345	228
$Au/Ce/SiO_2$-i	36	5.1	2.45	365	271
$Au/Ce/SiO_2$-s	31	5.7	2.69	271	205
$Au/Fe/SiO_2$-i	36	5.2	2.52	459	195
$Au/Fe/SiO_2$-s	26	6.4	2.81	422	214
$Au/La/SiO_2$-i	35	5.3	2.64	242	142
$Au/La/SiO_2$-s	32	5.5	2.59	325	110

The reaction mixture was stirred in a semibatch reactor operated under atmospheric pressure at 80 °C. Oxygen was bubbled through the suspension with a flow rate of 30 mL/min for 6 h. To monitor the reaction progress, small aliquots were taken from the reactor at different intervals of time and at the end of the test, using a syringe with nylon filters (pore 0.45 μm), and were analyzed by GC in a Varian 450 GC, using a capillary DB wax column (15 m × 0.548 mm), He as the carrier gas and a FID detector. In all measurements the carbon balance was within 100 ± 3%. Prior to tests, catalyst samples were prereduced with pure H_2 (10 mL/min) at 300 °C for 1 h.

3. Results and discussion

The chemical composition and S_{BET} of samples and bare supports are presented in Table 1. EDS results showed that Au content was similar in all gold-containing samples. Modification of the support with Fe, Ce and La oxides by both methods lead to change in structural characteristics; however, these changes are not critical. Deposition of gold decreases S_{BET} in all samples as a result of partial blocking the support pores; this effect is normally observed in all porous systems.

Pure SiO_2 and M/SiO_2-*s* samples prepared by direct synthesis showed similar XRD patterns (Fig. 1). This implies that either the modifier forms an amorphous phase in the *s*-supports, or that the modifier particles size is below the XRD detection limit (Fig. 2a). Regarding the *i*-supports, the peaks corresponding to CeO_2 and Fe oxides (Fe_2O_3 and Fe_3O_4), phases were observed only for Ce/SiO_2-*i* and Fe/SiO_2-*i*. Hence, supports modification with Ce and Fe oxides by impregnation was not successful, i.e., they are partially agglomerated on the surface of the silica support rather than evenly distributed along the entire support. Interestingly, iron oxide phases disappear after gold deposition because of surface components redistribution (Fig. 1b). In the case of modification with La by both methods, peaks of La-containing phases were not observed, probably due to their high dispersion in the silica support.

XRD patterns of Au/SiO_2, $Au/Ce/SiO_2$-*i*, $Au/Ce/SiO_2$-*s* and $Au/Fe/SiO_2$-*i* (Fig. 1b) showed a reflection at $2\theta = 38^\circ$ with very low intensity, corresponding to the (1 1 1) plane of metallic Au. Table 2 presents content and size of crystalline gold estimated by Rietveld refinement methods for these XRD patterns. The broad FWHM of the diffraction peak for SiO_2 at $2\theta \sim 22$–26° indicates the small particle size of SiO_2; it is in good agreement with diameter observed by HRTEM (2–4 nm) [48]. The absence of modifier diffraction peaks indicate that the modifiers were homogeneously distributed in most of the studied Au-based samples.

XRD results indicate that, in general, direct synthesis method (*s*) provides a better modifier distribution on the silica surface than impregnation method (*i*). Modification of silica support by impregnation of CeO_2 was not achieved even after gold deposition. Thus, we could expect that $Au/Ce/SiO_2$-*i* sample show catalytic properties similar to unmodified Au/SiO_2.

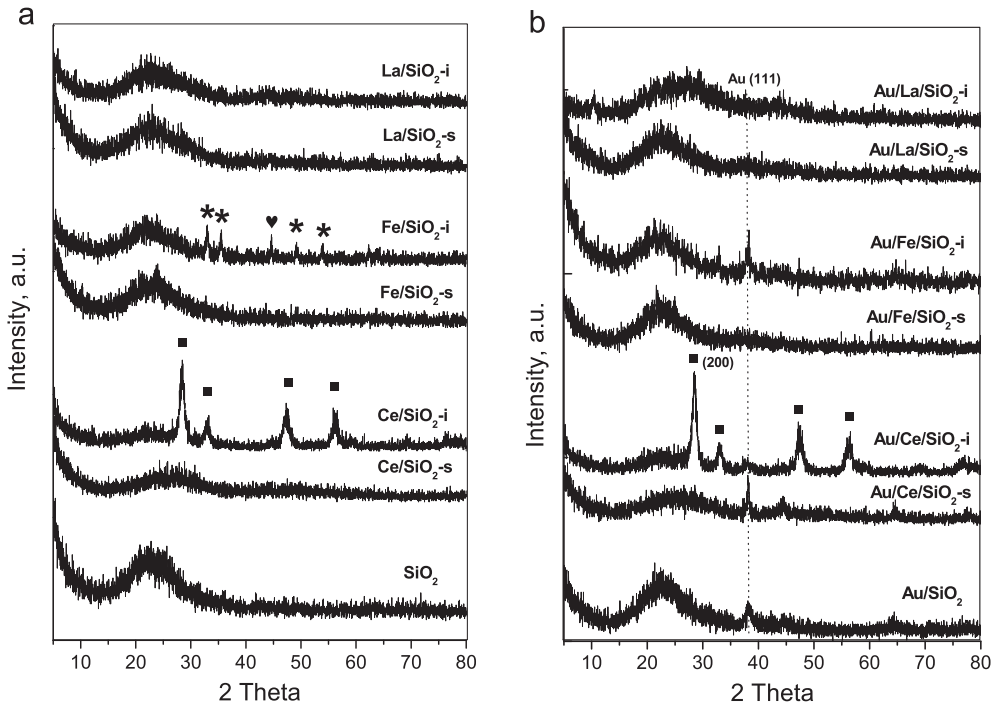

Fig. 1. XRD patterns for supports (a) and gold-containing samples (b) after H_2 treatment at 300 °C for 1 h Symbols: ■ CeO_2; * Fe_2O_3; ♥ Fe_3O_4.

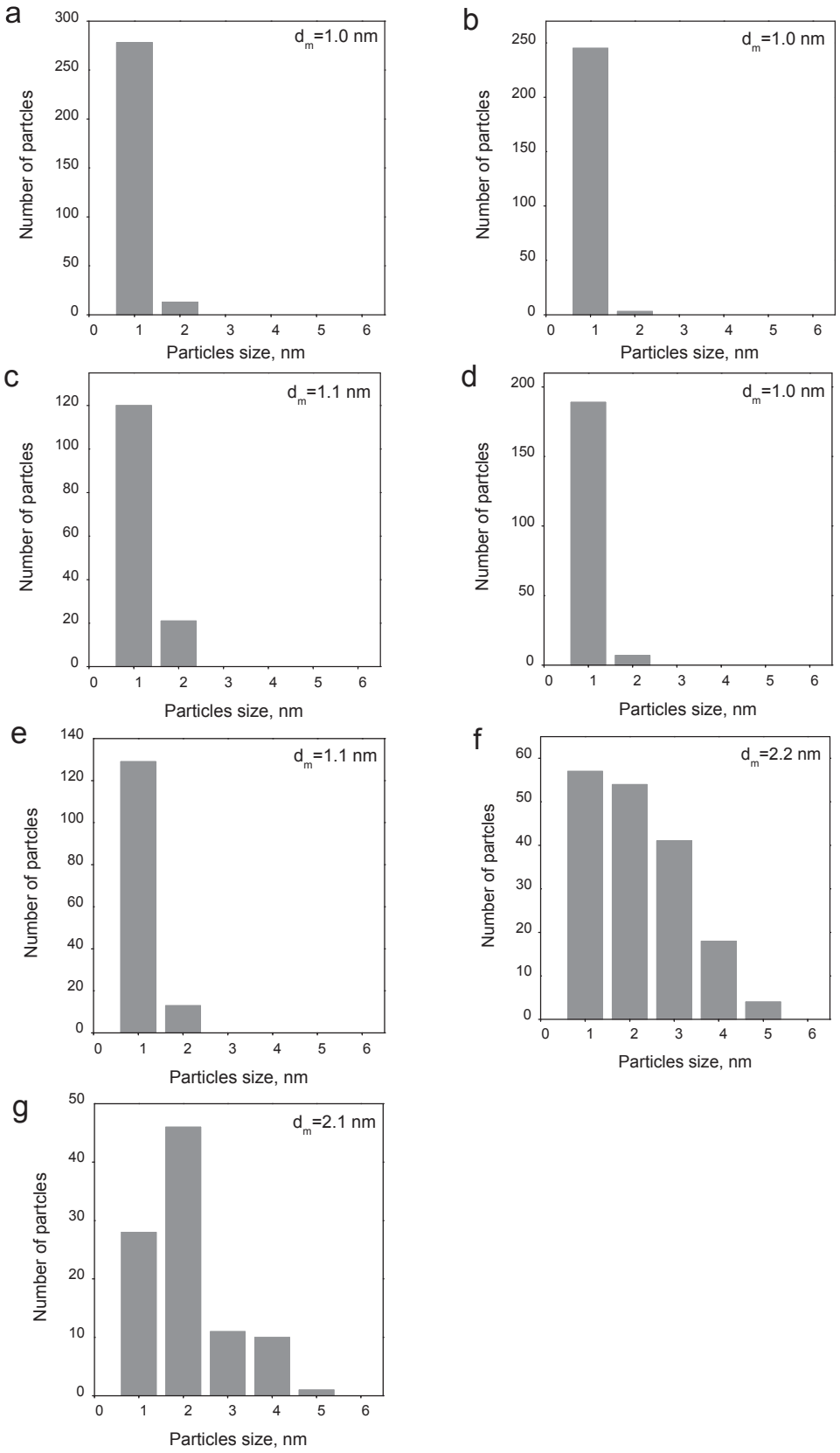

Fig. 2. Au NPs size distribution obtained by HRTEM for samples: Au/La/SiO_2-*s* (a), Au/La/SiO_2-*i* (b), Au/Fe/SiO_2-*s* (c), Au/Fe/SiO_2-*i* (d), Au/Ce/SiO_2-*s* (e), Au/Ce/SiO_2-*i* (f) and Au/SiO_2 (g).

Table 2
Gold crystal size and content estimated by Rietveld refinement methods.

Sample	Au crystal size (nm)	Au crystalline phase	
		wt%	% of total Au content
Au/SiO_2	14	1.1	44
$Au/Ce/SiO_2$-i	7	1.5	61
$Au/Ce/SiO_2$-s	25	1.0	37
$Au/Fe/SiO_2$-i	15	0.9	34

Gold particle size distributions (Fig. 2) estimated from HRTEM images of the samples (Fig. 3) show that the diameter of Au particles was ≤2 nm, with a maximum at ~1 nm for most of the studied samples. The particle size distribution for Au/SiO_2 and $Au/Ce/SiO_2$-*i* was relatively broad (1–4 nm) with the average particle size 2 nm, while for the other samples the distribution was quite narrow, with up to 85.1, 95.5 and 98.8% of particles having a diameter of 1 nm for $Au/Fe/SiO_2$-*i*, $Au/La/SiO_2$-*s* and $Au/La/SiO_2$-*i*, respectively. Only $Au/Fe/SiO_2$-*s*, $Au/La/SiO_2$-*s* and $Au/La/SiO_2$-*i* showed a monodisperse distribution of the gold particles of 1 nm. The sample $Au/Ce/SiO_2$-*i* is out of consideration because, besides Au crystalline phase (crystalline size calculated by Rietveld refinement was 7 nm), it includes CeO_2 crystalline phase (8.4 nm). Au and CeO_2 have close contrast in HRTEM [54,55] and crystalline size (Table 2), which makes it difficult to distinguish between Au and CeO_2 NPs. Detailed HRTEM images of the 2–5 nm bare supports are reported in [48].

Leaving aside the monodispersity issue, there are scarce reports on the synthesis of supported small particles on ultra-small silica. To our knowledge, only two methods of obtaining gold nanoparticles of 1 nm are previously described in the literature [43–45]. Tsukuda's group [43,44] prepared small Au NPs (~1 nm) from pre-formed Au NPs stabilized by polymers, yielding a product with very low loading of active metal (0.07% wt. Au). Strictly speaking, the study of the Au NPs properties in this system is impossible, because their surface is substantially blocked by a stabilizing polymer. Yang's group [45] reported synthesis of small Au NPs (~1 nm) covering the SiO_2 support surface with less inert graphene oxide nanosheets.

In those two articles, the materials based on gold nanoparticles were obtained at low temperatures (100 °C). In the present study the samples were prepared at 300 °C; which proves that our Au NPs were stable at higher temperatures than those reported in the literature. Stability of Au NPs is very important factor for obtaining effective gold catalysts because aggregation of the nanoparticles is one of the main reasons of gold catalyst deactivation during performance and storage [46,47].

Thus, based on XRD and HRTEM data, we can conclude that 1 nm Au NPs were obtained due to modification of silica with the transition metal oxides. Introduction of the modifier basically increased the interaction of gold with the support surface. The modification by direct incorporation during direct synthesis provided a stronger interaction of gold with support than the impregnation. The most promising modifier for obtaining the monodisperse samples is La oxide. Methods of preparation of 1 nm Au NPs on silica reported in the literature include complete isolation of the support surface or gold surface to optimize gold-support interaction [42–44]. These methods of formation of small Au NPs on an inert support are much longer and more expensive than the one described in the present work. In addition, samples obtained in this work are stable at much higher temperatures.

Catalytic oxidation of 1-octanol under very mild conditions was used to test the influence of the support modification on the catalytic redox properties of the monodispersed Au NPs. Looking for accordance to green chemistry principles, the reaction was investigated at a relatively low temperature (80 °C) under atmospheric pressure using oxygen as oxidant, and without the use of base with the solvent. The substrate to metal ratio, i.e., the octanol/Au ratio, was selected to keep differential conditions in order to avoid or, at least, to minimize the effect of the secondary reactions. In the conditions explored, the main product of 1-octanol selective oxidation on every tested supported gold catalyst was octanol, being the ester (octyl octanoate) the only subproduct. No acid formation was detected in any case. The evolution of the reaction with time is shown in Fig. 4a where some results from [33] are included for comparative purposes.

The highest initial rates, around threefold bigger than that on the unmodified Au/SiO_2 and practically equal among them, were observed for catalysts $Au/Fe/SiO_2$-i, $Au/Ce/SiO_2$-i and $Au/Fe/SiO_2$-s. On the contrary, the lowest was observed for catalyst $Au/Ce/SiO_2$-s. Activity evolution with run time was different among the catalysts. During the reaction time explored, the rate of 1-octanol oxidation on Au/SiO_2 and the four catalysts modified with La and Ce remained stable. On the contrary, Fe-modified samples showed some deactivation: the method of preparation had drastic effect on their catalytic properties for the samples modified with Fe: initial rate of $Au/Fe/SiO_2$-*i* decreased slowly with time, while $Au/Fe/SiO_2$-*s* deactivated very fast, and conversion practically did not change after 2 h of reaction. After this run time, product distribution changed drastically (Fig. 4b), with a much higher formation of the ester, which points to a possible change in the nature of the surface centers. As a consequence, Ce and Fe-modified catalysts prepared by direct synthesis were the less active ones after 6 h. This result evidences also the need to follow the evolution of activity with run time when investigating this type of reaction, an aspect frequently overlooked when comparing catalysts in the literature. For both La-modified samples the effect of the additive affected only product distribution regardless the method of modification; their catalytic properties were very close to those of Au/SiO_2. Thus, the best performance was found with impregnated Ce-modified support, with the highest conversion and stability, and the relative order of activity was: $AuCeSiO_2$-*i* > $AuFeSiO_2$-*i* ≫ $AuLaSiO_2$-*i* ≈ $AuLaSiO_2$-*s* > $AuSiO_2$ > $AuFeSiO_2$-*s* ≫ $AuCeSiO_2$-*s*.

Influence of electronic state (effective charge) of gold on its catalytic properties is well-known and described in literature [9,56–67]. In general, redox catalysis can be considered as a multiple repetition of oxidation-reduction cycles on the active sites. Changes in electronic state (effective charge) of supported gold systems as a result of metal-support interaction are the main reason to use specifically supported rather than free Au NPs. According to our previous results supported gold ions Au^+ and charged clusters $Au_n^{\delta+}$ are active sites of gold catalysts in oxidation processes [30–33,46,47]. Particularities of formation and stabilization of different gold states in the studies systems were investigated by FTIR of adsorbed CO.

FTIR spectra of adsorbed CO were registered in the typical range where the different electronic states of gold species are observed (2000–2250 cm^{-1}) after H_2 or O_2 pretreatments. They are presented in a Fig. 5, arranged in order of descending of catalytic activity, spectra of monodisperse gold samples are marked with grey background sample name. CO adsorption on pure supports was not detected in this range. At the room temperature CO is adsorbed only on NPs of size ≤2 nm [69], and small particles are sensitive to pretreatment conditions [47,54,68]. Thus, only the active surface of Au was studied by FTIR of absorbed CO. Data for spectra interpretation, taken from literature [59–67] and our previous studies [55–58,68], are summarized in Table 3 where data for monodisperse gold samples are marked with grey background.

In previous studies it was have shown that the maximum activity in CO oxidation and in the liquid-phase alcohol oxidation of supported gold catalysts is correlated with the presence of gold in Au^+ and $Au_n^{\delta+}$ states [57–59,69,70]. All the samples studied here were characterized by Au^0 formation after H_2-treatment (absorption bands at 2100–2120 cm^{-1} attributed to Au^0-CO carbonyl complexes on small Au NPs). After oxidizing treatment with O_2 these bands disappeared, obviously, because of oxidation of such small NPs or their thermal aggregation to bigger metal particles, on which CO is not adsorbed at ambient temperature. After O_2-treatment partly charged states $Au^{\delta+}$

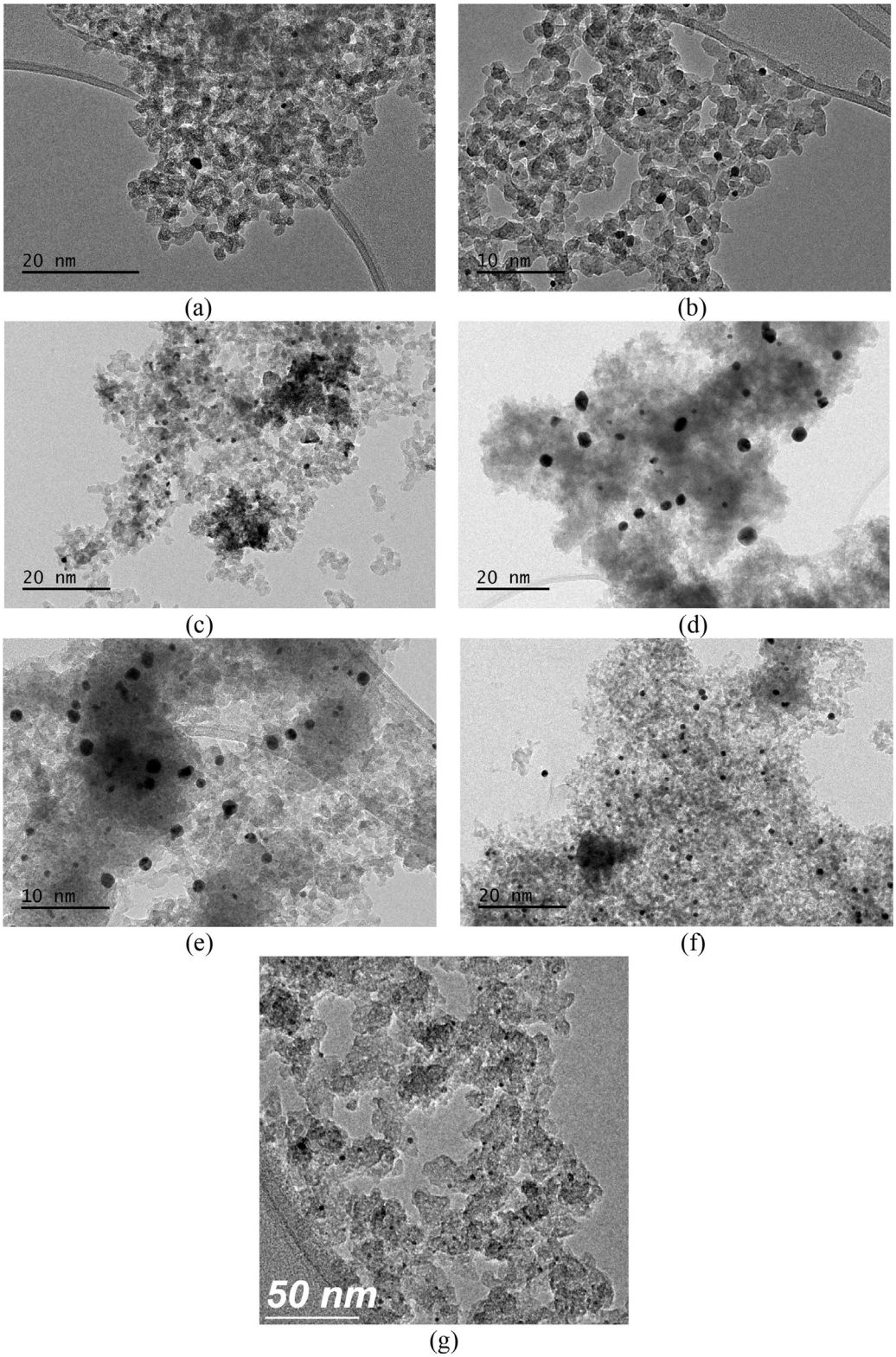

Fig. 3. Representative HRTEM micrographs of samples Au/La/SiO_2-*s* (a), Au/La/SiO_2-*i* (b), Au/Fe/SiO_2-*s* (c), Au/Fe/SiO_2-*i* (d), Au/Ce/SiO_2-*s* (e), Au/Ce/SiO_2-*i* (f) and Au/SiO_2 (g).

(absorption bands at 2125–2145 cm^{-1} attributed to $Au^{\delta+}$–CO carbonyl complexes with different effective charge) were observed for two Fe-modified samples, Au/Ce/SiO_2-*s* and Au/La/SiO_2-*s*, but not for Au/Ce/SiO_2-*i,* Au/La/SiO_2-*i* and Au/SiO_2. Thus, some modifiers can favor and stabilize formation of these electronic states of supported gold. It is an important result because, according to our previous studies, these are the active states of gold in redox catalytic processes.

It is interesting to note that in 1-octanol oxidation the method of modification matters while Au NPs dispersity neither electronic states of supported gold do not show any clear correlation with catalytic properties. The reason could be the increased importance of interaction of heavy massive molecule of the reactant with a catalyst surface, which

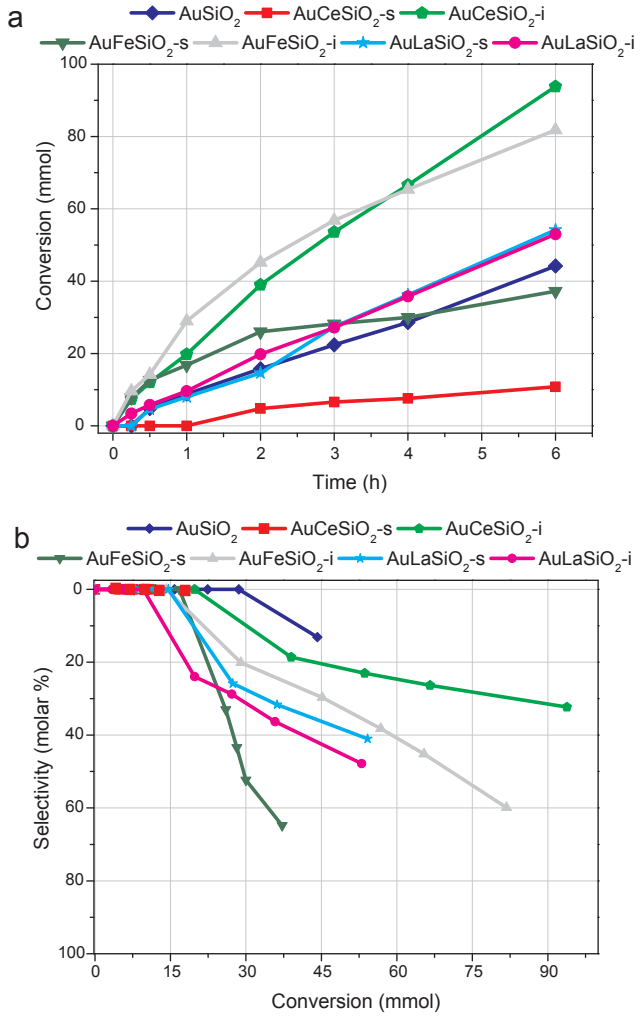

Fig. 4. Effect of the support on catalytic properties of studied Au catalysts in 1-octanol oxidation: conversion (a) and selectivity evolution with conversion (b). Reaction conditions: 0.1 M 1-octanol in n-heptane, no base added; T = 80 °C, molar ratio octanol/Au = 100. The results are partially taken from [33].

is determined by the nature, content and electronic state of the additive, which depend on the modification process parameters. It is known that each of used modifiers characterized with different adsorption properties (depends on metal-support interaction, acid-basic sites, electronic states etc.), oxygen mobility and oxygen storage capacity [71–74]. Among other supports CeO_2 has been widely used in oxidation reactions due to its oxygen mobility and storage capacity, which allow the formation of Ce^{3+} sites and adsorbed oxygen species due to metal-support interactions [75–79]. It is anticipated that CeO_2 phase formed in Au/Ce/SiO_2-*i* may play decisive role in its high catalytic activity [80]. Further experiments should be done to clarify the mechanism of modifier influence on 1-octanol oxidation.

4. Conclusions

A new approach for formation of small Au nanoparticles on SiO_2 support was proposed. It consists in application of ultra-small SiO_2 nanoparticles (2–4 nm) as a support and modification of their surface with other oxides having a stronger metal-support interaction with gold, which permits to obtain Au particles with high degree of monodispersity and stable when treated in H_2 up to 300 °C.

Modification of support surface with additives typically applied for increasing metal-support interaction (Fe, Ce and La oxides) led to changes in textural properties of the support (S_{BET}) and supported metal particle size distribution. XRD results indicate that incorporation of the metal oxide promotors by direct synthesis method provides a better modifier distribution on the surface of silica than impregnation method.

Modification with La by both methods and with Fe by impregnation method led to formation of 1 nm monodispersed Au nanoparticles. Modifiers change electronic properties of supported gold; they favor formation and stabilization of $Au^{\delta+}$ states, which are probable active sites of gold catalysts in redox catalytic processes.

The best performance for 1-octanol oxidation (as a model reaction for biomass alcohols fatty oxidation) was found for gold supported on impregnated Ce-modified support, with the highest conversion and

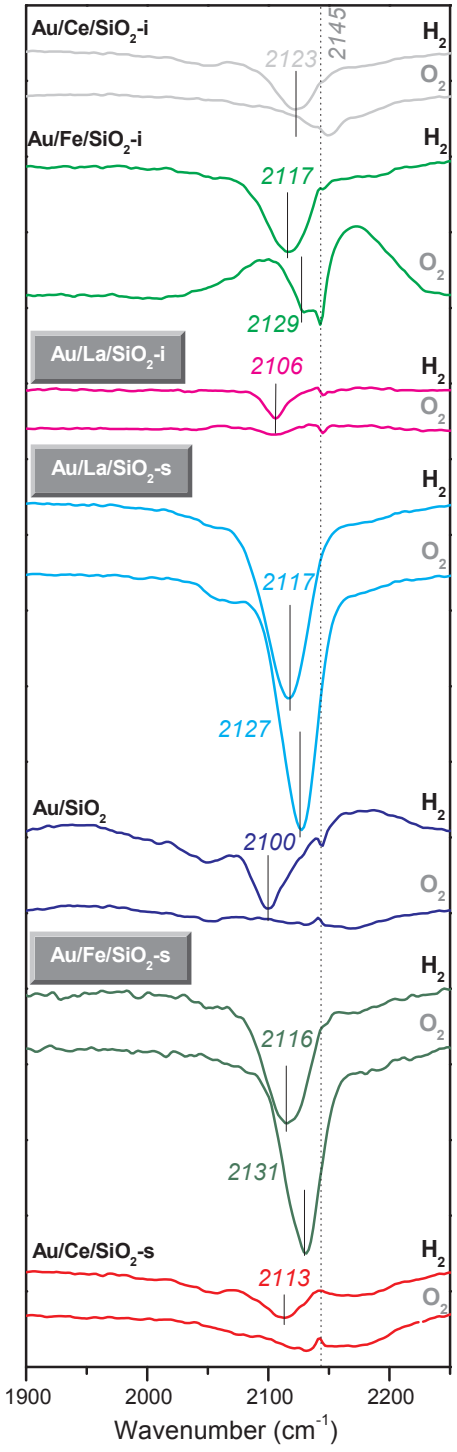

Fig. 5. FTIR spectra of CO adsorbed on Au NPs catalysts pretreated in H_2 or O_2.

Table 3
Experimental CO adsorption bands in FTIR for gold-containing samples after H_2 or O_2 pretreatment at 300 °C for 1 h.

Sample	Au^0-CO 2080–2120, (cm^{-1})		$Au^{\delta+}$–CO 2125–2145, (cm^{-1})	
	H_2	O_2	H_2	O_2
Au/Ce/SiO_2-i	2123	–	–	–
Au/Fe/SiO_2-i	2117	–	–	2129
Au/La/SiO_2-i	2106	2106	–	–
Au/La/SiO_2-s	2117	–	–	2127
Au/SiO_2	2100	–	2129	–
Au/Fe/SiO_2-s	2116	–	–	2131
Au/Ce/SiO_2-s	2113	–	–	2132

reaction rate stability, and the relative order of activity was: AuCeSiO$_2$-*i* > AuFeSiO$_2$-*i* ≫ AuLaSiO$_2$-*i* ≈ AuLaSiO$_2$-*s* > AuSiO$_2$ > AuFeSiO$_2$-*s* ≫ AuCeSiO$_2$-*s*. The obtained results open the possibility of further development of high-performance catalysts for conversion of secondary products of biomass processing into valuable chemicals.

Acknowledgements

This work is funded by CONACYT projects 279889, 1073, 293418, 1216 and PAPIIT-UNAM projects IN105416, IN112117 and IN107715; PAPITE-UNAM projects PE101517 and PE101317 (Mexico); Tomsk Polytechnic University Competitiveness Enhancement Program (Russia), grant VIU-ISCBMT-196/2018; and MINECO project CTQ2017-86170-R (Spain). We also thank LINAN-IPICyT for providing access to databases. We gratefully thank E. Flores, Sh. Sandoval, I. Gradilla, J. Mendoza, E. M. Aparicio, J.A. Peralta, M. Sainz, P. Casillas Figueroa, R. Vélez, J. E. Cabrera Ortega, R. González Pedraza, Dr. M. Farías, R. Luna Vazques and M.I. Perez for valuable technical assistance.

References

[1] Zhao GF, Ling M, Hu HY, Deng MM, Xue QS, Lu Y. An excellent Au/meso-gamma-Al(2)O(3) catalyst for the aerobic selective oxidation of alcohols. Green Chem 2011;13:3088–92.
[2] Fu Q, Saltsburg H, Flytzani-Stephanopoulos M. Active nonmetallic Au and Pt species on ceria-based water-gas shift catalysts. Science 2003;301:935–8.
[3] Chowdhury B, Bravo-Suárez JJ, Mimura N, Jiqing L, Bando KK, Tsubota S, et al. In situ UV-Vis and EPR study on the formation of hydroperoxide species during direct gas phase propylene epoxidation over Au/Ti-SiO_2 catalyst. J Phys Chem B 2006;110:22995–9.
[4] Karthika V, Arumugam A, Gopinath K, Kaleeswarran P, Govindarajan M, Alharbi NS, et al. Guazuma ulmifolia bark-synthesized Ag, Au and Ag/Au alloy nanoparticles: photocatalytic potential, DNA/protein interactions, anticancer activity and toxicity against 14 species of microbial pathogens. J Photochem Photobiol B 2017;167:189–99.
[5] Ding X, Yuan P, Gao N, Zhu H, Yang YY, Xu Q-H. Au-Ag core-shell nanoparticles for simultaneous bacterial imaging and synergistic antibacterial activity. Nanomed-Nanotechnol 2017;13:297–305.
[6] Vial S, Reis RL, Oliveira JM. Nanoparticles for bone tissue engineering. Biotechnol Prog 2017;33(3):590–611.
[7] Liang YR, Zhang ZM, Liu ZJ, Wang K, Wu XY, Zeng K, et al. A highly sensitive signal-amplified gold nanoparticle-based electrochemical immunosensor for dibutyl phthalate detection. Biosens Bioelectron 2017;91:199–202.
[8] Caetano FR, Felippe LB, Zarbin AJG, Bergamini MF, Marcolino-Jr LH. Gold nanoparticles supported on multi-walled carbon nanotubes produced by biphasic modified method and dopamine sensing application. Sensor Actuat B-Chem 2017;243:43–50.
[9] Qina L, Zeng G, Lai C, Huang D, Zhang C, Xu P, et al. A visual application of gold nanoparticles: simple, reliable and sensitive detection of kanamycin based on hydrogen-bonding recognition. Sensor Actuat B-Chem 2017;243:946–54.
[10] Esmaeili C, Heng LY, Chiang CP, Rashid ZA, Safitri E, Malon Marugan RSP. A DNA biosensor based on kappa-carrageenan-polypyrrole-gold nanoparticles composite for gender determination of Arowana fish (Scleropages formosus). Sensor Actuat B-Chem 2017;242:616–24.
[11] Zhai Y, Wang Q, Qi Z, Li C, Xia J, Li X. Experimental investigation of energy transfer between CdSe/ZnS quantum dots and different-sized gold nanoparticles. Physica E 2017;88:109–14.
[12] Zhou Y, Ma Z. Colorimetric detection of Hg2+ by Au nanoparticles formed by H_2O_2 reduction of $HAuCl_4$ using Au nanoclusters as the catalyst. Sensor Actuat B-Chem 2017;241:1063–8.
[13] Arrii S, Morfin F, Renouprez J, Rousset JL. Oxidation of CO on gold supported catalysts prepared by laser vaporization: direct evidence of support contribution. J Am Chem Soc 2004;126:1199–205.
[14] Lopez N, Janssens TVW, Clausen BS, Xu Y, Mavrikakis M, Bligaard T, et al. J Catal 2004;223:232–5.
[15] Yuan Y, Kozlova AP, Asakura K, Wan H, Tsai K, Iwasawa Y. Supported Au catalysts prepared from Au phosphine complexes and as-precipitated metal hydroxides: characterization and low-temperature CO oxidation. J Catal 1997;170:191–9.
[16] Kozlov AI, Kozlova AP, Asakura K, Matsui Y, Kogure T, Shido T, et al. Supported gold catalysts prepared from a gold phosphine precursor and as-precipitated metal-hydroxide precursors: effect of preparation conditions on the catalytic performance. J Catal 2000;196:56–65.
[17] Grunwaldt JD, Kiener C, Wögerbauer C, Baiker A. Preparation of supported gold catalysts for low-temperature CO oxidation via "Size-Controlled" gold colloids. J Catal 1999;181:223–32.
[18] Haruta M, Tsubota S, Kobayashi T, Kageyama H, Genet MJ, Delmon B. Low-temperature oxidation of CO over gold supported on TiO_2, α-Fe_2O_3, and Co_3O_4. J Catal 1993;144:175–92.
[19] Valden M, Lai X, Goodman DWW. Onset of catalytic activity of gold clusters on Titania with the appearance of nonmetallic properties. Science 1998;281:1647–50.
[20] Mavrikakis M, Stoltze P, Nørskov JK. Making gold less noble. Catal Lett 2000;64:101–6.
[21] Mallick K, Witcomb MJ, Scurrell MS. Supported gold catalysts prepared by in situ reduction technique: preparation, characterization and catalytic activity measurements. Appl Catal A Gen 2004;259:163–8.
[22] Veith GM, Lupini AR, Rashkeev S, Pennycook SJ, Mullins DR, Schwartz V, et al. Chromium catalyzed tetramerization of ethylene in a continuous tube reactor-proof of concept and kinetic aspects. J Catal 2009;262:92–101.
[23] Zhu H, Ma Z, Clark JC, Pan Z, Overbury SH, Dai S. Low-temperature CO oxidation on Au/fumed SiO_2-based catalysts prepared from $Au(en)_2Cl_3$ precursor. Appl Catal, A 2007;326:89–99.
[24] Somodi F, Borbáth I, Hegedűs M, Tompos A, Sajó IE, Szegedi Á, et al. Modified preparation method for highly active Au/SiO_2 catalysts used in CO oxidation. Appl Catal A 2008;347:216–22.
[25] Budroni G, Corma A. Gold–organic–inorganic high-surface-area materials as precursors of highly active catalysts. Angew Chem Int Ed 2006;45:3328–31.
[26] Villa A, Dimitratos N, Chan-Thaw CE, Hammond C, Prati L, Hutchings GH. Glycerol oxidation using gold-containing catalysts. Acc Chem Res 2015;48:1403–12.
[27] Carrettin S, McMorn P, Johnston P, Griffin K, Kiely CJ, Hutchings GJ. Oxidation of glycerol using supported Pt, Pd and Au catalysts. Phys Chem Chem Phys 2003;5:1329–36.
[28] Sobczak I, Wolski Ł. Au-Cu on Nb_2O_5 and Nb/MCF supports - surface properties and catalytic activity in glycerol and methanol oxidation. Catal Today 2015;254:72–82.
[29] Musialska K, Finocchio E, Sobczak I, Busca G, Wojcieszak R, Gaigneaux E, et al. Characterization of alumina- and niobia-supported gold catalysts used for oxidation of glycerol. Appl Catal A 2010;384:70–7.
[30] Kotolevich Y, Kolobova E, Khramov E, Farías MH, Zubavichus Y, Tiznado H, et al. n-Octanol oxidation on Au/TiO_2 catalysts promoted with La and Ce oxides. Mol Catal 2017;427:1–10.
[31] Kotolevich Y, Kolobova E, Mamontov G, Khramov E, Cabrera Ortega JE, Tiznado H, et al. Au/TiO_2 catalysts promoted with Fe and Mg for n-octanol oxidation under mild conditions. Catal Today 2016;278:104–12.
[32] Kotolevich Y, Kolobova E, Pestryakov A, Zanella R, Zubavichus Y, Khramov E, et al. Gold and silver catalysts for liquid phase *n*-octanol oxidation: effect of promoters. Curr Org Synt 2017;14(3):323–31.
[33] Martínez-González S, Gómez-Avilés A, Martynyuk O, Pestryakov A, Bogdanchikova N, Cortés Corberán V. Selective oxidation of 1-octanol over gold supported on mesoporous metal-modified HMS: the effect of the support. Catal Today 2014;227:65–70.
[34] Gluhoi AC, Vreeburg HS, Bakker JW, Nieuwenhuys BE. Activation of CO, O_2 and H_2 on gold-based catalysts. Appl Catal A 2005;291:145–50.
[35] Lippits MJ, Gluhoi AC, Nieuwenhuys BE. A comparative study of the selective oxidation of NH_3 to N_2 over gold, silver and copper catalysts and the effect of addition of Li_2O and CeOx. Catal Today 2008;137:446–52.
[36] Lippits MJ, Gluhoi AC, Nieuwenhuys BE. A comparative study of the effect of addition of CeO x and Li_2O on γ-Al_2O_3 supported copper, silver and gold catalysts in the preferential oxidation of CO. Top Catal 2007;44:159–65.
[37] Gluhoi AC, Nieuwenhuys BE. Structural and chemical promoter effects of alkali (earth) and cerium oxides in CO oxidation on supported gold. Catal Today 2007;122:226–32.
[38] Gluhoi AC, Tang X, Marginean P, Nieuwenhuysa BE. Characterization and catalytic activity of unpromoted and alkali (earth)-promoted Au/Al_2O_3 catalysts for low-temperature CO oxidation. Top Catal 2006;39:101–10.
[39] Shiraishi Y, Tanaka H, Sakamoto H, Ichikawac S, Hiraia T. Photoreductive synthesis of monodispersed Au nanoparticles with citric acid as reductant and surface stabilizing reagent. RSC Adv 2017;7:6187–92.
[40] Shiraishi D, Mutreja I, Sykes P. Seed mediated synthesis of highly mono-dispersed gold nanoparticles in the presence of hydroquinone. Nanotechnology 2016;27:14.
[41] Abdelghany AM, Mekhail MS, Abdelrazek EM, Aboud MM. Combined DFT/FTIR structural studies of monodispersed PVP/Gold and silver nano particles. J Alloys Compd 2015;646:326–32.
[42] Huang Y, Liu W, Yang L, Huang T, Jiang Y, Yao T, et al. XAFS study on structural order in highly monodispersed thiol-stabilized Au nanoparticles. J Phys Conf Ser 2016;712:012066.
[43] Liu Y, Tsunoyama H, Akita T, Tsukuda T. Preparation of ~1 nm gold clusters confined within mesoporous silica and microwave-assisted catalytic application for alcohol oxidation. J Phys Chem C 2009;113:13457–61.

[44] Yamazoe S, Koyasu K, Tsukuda T. Nonscalable oxidation catalysis of gold clusters. Acc Chem Res 2014;47:816–24.
[45] Peng L, Zhang J, Yang S, Han B, Sang X, Liu C, et al. Ultra-small gold nanoparticles immobilized on mesoporous silica/graphene oxide as highly active and stable heterogeneous catalysts. Chem Commun 2015;51:4398–401.
[46] Bogdanchikova N, Pestryakov A, Tuzovskaya I, Zepeda TA, Farias MH, Tiznado H, et al. Effect of redox treatments on activation and deactivation of gold nanospecies supported on mesoporous silica in CO oxidation. Fuel 2013;110:40–7.
[47] Martynyuk O, Kotolevich Y, Vélez R, Cabrera Ortega JE, Tiznado H, Zepeda T, et al. On the high sensitivity of the electronic states of 1 nm gold particles to pretreatments and modifiers. Molecules 2016;21:432.
[48] Martynyuk O, Kotolevich Y, Pestryakov A, Mota-Morales JD, Bogdanchikova N. Nanostructures constituted by unusually small silica nanoparticles modified with metal oxides as support for ultra-small gold nanoparticles. Colloids Surfaces A Physicochem Eng Asp 2015;487:9–16.
[49] Tanev PT, Chibwe M, Pinnavaia TJ. Titanium-containing mesoporous molecular sieves for catalytic oxidation of aromatic compounds. Nature 1994;368:321–3.
[50] Tanev PT, Pinnavaia TJ. A neutral templating route to mesoporous molecular sieves. Science 1995;267:865–7.
[51] Smolentseva E, Bogdanchikova N, Simakov A, Pestryakov A, Tusovskaya I, Avalos M, et al. Influence of copper modifying additive on state of gold in zeolites. Surf Sci 2006;600:4256–9.
[52] Zanella R, Delannoy L, Louis C. Mechanism of deposition of gold precursors onto TiO_2 during the preparation by cation adsorption and deposition–precipitation with NaOH and urea. Appl Catal A 2005;291:62–72.
[53] Parreira LA, Bogdanchikova N, Pestryakov A, Zepeda TA, Tuzovskaya I, Farías MH, et al. Nanocrystalline gold supported on Fe-, Ti- and Ce-modified hexagonal mesoporous silica as a catalyst for the aerobic oxidative esterification of benzyl alcohol. Appl Catal A: Gen 2011;397:145–52.
[54] Arena F, Famulari P, Trunfio G, Bonura G, Frusteri F, Spadaro L. Probing the factors affecting structure and activity of the Au/CeO_2 system in total and preferential oxidation of CO. Appl Catal B: Environ 2006;66:81–91.
[55] Avgouropoulos G, Manzoli M, Boccuzzi F, Tabakova T, Papavasiliou J, Ioannides T, et al. Catalytic performance and characterization of Au/doped-ceria catalysts for the preferential CO oxidation reaction. J Catal 2008;256:237–47.
[56] Kolobova E, Kotolevich Y, Pakrieva E, Mamontov G, Farías MH, Bogdanchikova N, et al. Causes of activation and deactivation of modified nanogold catalysts during prolonged storage and redox treatments. Molecules 2016;21:486.
[57] Gruver V, Fripiat JJ. Lewis acid sites and surface aluminum in aluminas and mordenites: an infrared study of CO chemisorption. J Phys Chem 1994;98:8549–54.
[58] Salama T. Characterization of gold(I) in NaY zeolite and acidity generation. J Catal 1995;152:322–30.
[59] Guillemot D, Borovkov VY, Kazansky VB, Polisset-Thfoin M, Fraissard J. Surface characterization of Au/HY by 129XeNMR and diffuse reflectance IR spectroscopy of adsorbed CO. Formation of electron-deficient gold particles inside HY cavities. J Chem Soc Faraday Trans 1997;93:3587–91.
[60] Reifsnyder SN, Otten MM, Lamb HH. Nucleation and growth of Pd clusters in mordenite. Catal Today 1998;39:317–28.
[61] Boccuzzi F, Chiorino A, Manzoli M, Andreeva D, Tabakova T. FTIR study of the low-temperature water-gas shift reaction on Au/Fe_2O_3 and Au/TiO_2. Catal J Catal 1999;188:176–85.
[62] Margitfalvi J, Fási A, Hegedűs M, Lónyi F, Gőbölös S, Bogdanchikova N. Au/MgO catalysts modified with ascorbic acid for low temperature CO oxidation. Catal Today 2002;72:157–69.
[63] Riahi G, Guillemot D, Polisset-Thfoin M, Khodadadi A, Fraissard J. Preparation, characterization and catalytic activity of gold-based nanoparticles on HY zeolites. Catal Today 2002;72:115–21.
[64] Mohamed MM, Mekkawy I. Electrical and chemical characteristics of nano-meter gold encapsulated in mesoporous and microporous channels and cages of FSM-16 and Y zeolites. J Phys Chem Solids 2003;64:299–306.
[65] Manzoli M, Chiorino A, Boccuzzi F. FTIR study of nanosized gold on ZrO_2 and TiO_2. Surf Sci 2003;532–535:377–82.
[66] Tabakova T, Boccuzzi F, Manzoli M, Andreeva D. FTIR study of low-temperature water-gas shift reaction on gold/ceria catalyst. Appl Catal A Gen 2003;252:385–97.
[67] Hernandez JA, Gómez S, Pawelec B, Zepeda TA. CO oxidation on Au nanoparticles supported on wormhole HMS material: effect of support modification with CeO_2. Appl Catal B Environ 2009;89:128–36.
[68] Tuzovskaya IV, Simakov AV, Pestryakov AN, Bogdanchikova NE, Gurin VV, Farías MH, et al. Catal Commun. 2007;8:977–80.
[69] Kolobova E, Kotolevich Y, Pakrieva E, Mamontov G, Farías MH, Bogdanchikova N, et al. Molecules 2016;21:486.
[70] Ampelli C, Barbera K, Centi G, Genovese C, Papanikolaou G, Perathoner S, et al. On the nature of the active sites in the selective oxidative esterification of furfural on Au/ZrO_2 catalysts. Catal Today 2016;278:56–65.
[71] Reina TR, Ivanova S, Centeno MA, Odriozola JA. Catalytic screening of Au/CeO_2-MOx/Al_2O_3 catalysts (M = La, Ni, Cu, Fe, Cr, Y) in the CO-PrOx reaction Int. J. Hydrog Energy 2015;40:1782–8.
[72] Fontanetti Nascimento L, FonsecaLima J, de Sousa Filho PC, Serra OA. Effect of lanthanum loading on nanosized CeO2-ZnO solid catalysts supported on cordierite for diesel soot oxidation J. Environ. Sci. - in press.
[73] Wang L, Huang M, Li B, Dong L, Jin G, Gao J, et al. Enhanced hydrothermal stability and oxygen storage capacity of La^{3+} doped CeO_2-γ-Al_2O_3 intergrowth mixed oxides. Ceram Int 2015;41:12988–95.
[74] Guo T, Liao H, Ge P, Zhang Y, Tian Y, Hong W, et al. Fe_2O_3 embedded in the nitrogen-doped carbon matrix with strong C-O-Fe oxygen-bridge bonds for enhanced sodium storages. Math Chem Phys 2018;216:58–63.
[75] Geonmonond RS, Quiroz J, Rocha GFSR, Oropeza FE, Rangel CJ, Rodrigues TS, et al. Marrying SPR excitation and metal-support interactions: unravelling the contribution of active surface species in plasmonic catalysis. Nanoscale 2018;10:8560.
[76] Zhou Y, Li S, Deng J, Xiong L, Wang J, Chen Y. Nanoscale heterogeneity and low-temperature redox property of CeO_2-ZrO_2-La_2O_3-Y_2O_3 quaternary solid solution. Math Chem Phys 2018;208:123–31.
[77] Reddy BM, Lakshmanan P, Bharali P, Saikia P, Thrimurthulu G, Muhler M, et al. Influence of alumina, silica, and titania supports on the structure and CO oxidation activity of $Ce_xZr_xO_2$ nanocomposite oxides. J Phys Chem 2007;111:10478–83.
[78] Reddy BM, Thrimurthulu G, Katta L, Yamada Y, Park S. Structural characteristics and catalytic activity of nanocrystalline ceria-praseodymia solid solutions. J Phys Chem C 2009;113:15882–90.
[79] Phokha S, Hunpratu S, Usher B, Pimsawat A, Chanlek N, Maensirid S. Effects of CeO_2 nanoparticles on electrochemical properties of carbon/CeO_2 composites. Appl Surf Sci 2018;446:36–46.
[80] Mukherjee D, Reddy BM. Noble metal-free CeO_2-based mixed oxides for CO and soot oxidation. Catal Today 2018;309:227–35.